INFLUENCE OF THE ATMOSPHERE ON THE THERMAL DECOMPOSITION KINETICS OF THE CaCO₃ CONTENT OF PFBC COAL FLYING ASH

M. A. Gabal[1]*, D. Hoff*[2] *and G. Kasper*[2]

[1]Chemistry Department, Faculty of Science, Benha University, Benha, Egypt
[2]Institut für Mechanische Verfahrenstechnik und Mechanik, Universität Karlsruhe, Germany

The thermal decomposition behavior of hard coal fly ash (HCA2), obtained from the combustion of an Australian hard coal in thermoelectric power plants, in different atmospheres (air, N_2 and N_2–H_2 mixture), was studied using thermogravimetry (TG), infrared-evolved gas analysis (IR-EGA), differential scanning calorimetry (DSC) and thermodilatometry (DIL) techniques. It was found that changing of the applied atmosphere affects the carbon content of the ash which results in different thermal decomposition behaviors. In air, the carbon content was oxidized to carbon dioxide before the decomposition of carbonate. In N_2 or in N_2–H_2 atmospheres, the carbon content acts as a spacer causing a fewer points of contact between calcium carbonate particles, thus increasing the interface area which results in a decrease of the carbonate decomposition temperature. Following the carbonate decomposition, the iron oxide content of the ash undergoes a reductive decomposition reaction with the unburned carbon. This oxidation-reduction reaction was found to be fast and go to completion in presence of the N_2–H_2 mixture than in the pure nitrogen atmosphere due to the reducing effect of the hydrogen.

The kinetics of the carbonate decomposition step, in air and N_2–H_2 mixture was performed under non-isothermal conditions using different integral methods of analysis. The dynamic TG curves obeyed the Avrami–Erofeev equation (A_2) in air, and phase boundary controlled reaction equation (R_2) in N_2–H_2 mixture. The change in the reaction mechanism and the difference in the calculated values of activation parameters with the change of the atmosphere were discussed in view of effect of the atmosphere on the carbon content of the ash.

Keywords: CaCO₃, coal fly ash, kinetics, thermal analysis, unburned carbon

Introduction

Fly ash is the principal by-product of coal combustion in the thermoelectric power plants. The main components of the fly ash are the silicon dioxide (SiO_2), calcium sulfate ($CaSO_4$), calcium carbonate ($CaCO_3$) and calcium oxide (CaO). However fly ash also contains several other oxides (e.g. Al_2O_3, Fe_2O_3 and MgO) and unburned carbon [1].

The physical and chemical properties of coal fly ashes, their large quantity and environmental impacts enable using them in many industrial branches [2, 3]. For example [4–6], if the content of the unburned carbon is below 5% fly ash may be a valuable raw material for the construction industry (e.g. production of concrete).

The carbon content will depend on the efficiency of the combustion process and will normally be in the range 2–5% although the fly ash in some cases may contain up to 20% carbon. Excessive amounts of the residual carbon dispersed in the fly ash means a significant loss of energy [1]. So, in the past few years [7–9], increased attention has been paid to the determination of the amount and the behavior of the carbon content of fly ashes during combustion using thermal analysis techniques. The thermal behavior of the unburned carbon in different types of fly ashes was followed in oxidizing, inert and combining inert/oxidizing atmosphere by Paya *et al.* [7].

All suitable technologies for burning a wide range of fuels in power plants have in common that they need a sufficient removal of particle from the hot exhaust gases. Particle filter media for high temperature applications are often ceramic or metallic surface filter. Unfortunately, their long term process stability and reliability is affected by chemical composition of the fly ash particles [10]. One of the most important problem in the filtration processes is the raise of the adhesive force of particles at high temperature [11] which causes the raise of the pressure drop and make the cleaning of the filter surface affects the performance of dust collector, especially the release of the ash from a filter element. Hemmer *et al.* [10] show that the thermal processes of unreacted residues in the fly ashes can affect the filtration process. For example the fine particles of calcium oxide formed as the result of thermal

---

decomposition of calcium carbonate content of the ash may lead to such problem with the used filter. Consequently, the thermal decomposition behavior of the carbonate content of the ash must be extensively studied to avoid such problems. Kanaoka *et al.* [11] have studied the adhesive properties of coal fly ash particles with different calcium carbonate content under different gases conditions such as air, N_2, CO_2 and N_2–CO_2 mixture up to 950°C. So, it is apparent that the study of the thermal decomposition behavior and kinetics of the carbonate content of fly ashes will give us information about the suitable conditions for the filtration processes.

The thermal decomposition kinetics of $CaCO_3$ has been studied intensively by a large number of authors over many years, thus one might assume that this reversible decomposition process could be considered as a text case for kinetic studies. However, the results showed that, there are many different values given for the activation energy and different mechanisms for the decomposition process. A statistical survey of the published values of the activation energies and the mechanisms has been carried out by Maciejewski [12].

The effect of changing the surrounding atmosphere on the decomposition kinetics of $CaCO_3$ has been investigated by many authors [13, 14]. Criado *et al.* [14] have studied the influence of CO_2 pressure on the thermal decomposition kinetics of $CaCO_3$. It was reported that, it is possible to obtain meaningful and reliable kinetic parameters from isothermal and non-isothermal data provided that pressure correction term is included in the kinetic equation. The effect of steam (H_2O) and carbon dioxide (CO_2) on the rates of calcite decomposition have been studied using dynamic X-ray diffraction (DXRD) [15]. It was shown that the observed enhancement effect of steam is related to its adsorptive properties which are faster and more significant than CO_2 adsorption. Dynamic kinetic analysis has been performed on $CaCO_3$ [16] using simultaneous TG/DSC measurements in both wet and dry flowing argon. The differences in the results were discussed in terms of the properties measured and the possible influence of the atmosphere on the structural nature of the solid product.

The effect of dilution with silica (SiO_2) on the kinetics of the thermal decomposition of $CaCO_3$ in N_2 atmosphere was studied using a relationship other than the Arrhenius equation by Dollimore *et al.* [17]. The D_4 mechanism was taken as the possible mechanism and the Arrhenius parameters were found to decrease with the addition of silica.

The thermal analysis techniques including TG, DTA, DSC and DIL are widely used in combustion research for the determination and understanding of various properties and the behavior of different fuels under a wide range of conditions and applications. The objectives of this work are to use the different thermal analysis techniques to get further information about the thermal behavior of the hard coal flying ash (HCA2) under different surrounding atmospheres and to study the effect of the unburned carbon on the decomposition behavior and kinetics of the calcium carbonate content of the ash. In this way valuable information about the interactions between gas and particle compositions leading to a better understanding of particle behavior during the filtration process can be obtained.

Experimental

Materials

The coal fly ash studied in this research (HCA2) is a combustion product of an Australian hard coal in the PFBC (pressurized fluidized bed combustion) thermoelectric power plants in Wakamatzu (Japan). The fly ash was crushed, homogenized in an agate mortar and sieved. The main diameter of the obtained fraction was 7.44 μm. Table 1 represents the chemical and the mineral composition of the ash. From the table it is apparent that the only chemical compounds which may undergo thermal changes under the applied conditions in the temperature range up to 1000°C are carbon, calcium carbonate and iron oxide.

Quartz SF500 powder was used after thoroughly grinding to clarify the DIL behavior of the quartz content of the sample.

Table 1 Chemical and mineral composition of HCA2

Chemical composition	Mass%±0.03
Na_2O	<0.1
K_2O	0.2
MgO	0.5
CaO	27.1
Al_2O_3	16
SiO_2	33
Fe_2O_3	2
SO_3	2.5
Cl_{total}	0.39
SO_4-sulfur	0.99
H_2O_{total}	0.5
C_{total}	6.5
Mineral phases	
$CaSO_4$	14
CaO	–
$CaCO_3$	12
$Ca(OH)_2$	–
MgO	–
Quartz	28
Fe_2O_3	9
Amorphous	64

Instrumental methods

The chemical and the mineral composition of the ash was analyzed using Atomic Absorption Spectroscopy (AAS, Polarized Zeeman Z-8000200 Hitachi) and Shimadzu ICPS-75000 Inductively Coupled Plasma Atomic Emission Spectrometer (ICP-AES).

The thermal behavior of the ash in an oxidizing, weak reducing as well as in an inert atmosphere was studied using TG, DSC and DIL techniques. Characterization of the evolved gas accompanying the thermal changes was made using FTIR spectroscopy. In all experiments, all the atmospheres are from Holox. Air was used as an oxidizing atmosphere, N_2–H_2 mixture (98% N_2+2% H_2) was used as a reducing atmosphere and N_2 gas (99.9%) was used as an inert atmosphere. In all cases, the flow rate of the gas was adjusted at 1.5 L h^{-1}.

TG results were obtained using Netzsch (TG 209) thermal analyzer. The test samples were placed in an alumina crucible, 0.1 cm^3 in volume, which is loosely covered. The experiments were performed on heating up to 1000°C at 10°C min^{-1}. The kinetic experiments were carried out under dynamic conditions using heating rates of 1, 2, 3, 5, 10°C min^{-1}. The sample mass was kept at about 17 mg in all experiments to minimize any possible influence of the sample mass and in order to assure linear heating rate and accurate temperature measurements. Each experiment was repeated three times to assure the reproducibility of results.

The volatile reaction products were analyzed using a Bruker FT-IR (Vector 22) spectrophotometry directly coupled with the TG instrument. The evolved gas was transferred through a stainless steel tube heated at 200°C. EGA curves as a function of temperature were analyzed to determine the characteristic IR absorption bands using OPUS 3.1 software program. The wavenumber of these bands was compared with IR standard reference data base [18] to identify the evolved gas.

DSC experiments were carried out using Netzsch DSC-409 up to 900°C. Highly sintered α-Al_2O_3 powder was used as a reference material.

DIL measurements were performed using a WSK Mess- und Technik (TMA model) up to 850°C. The ash in a powdered form was pressed into pellets of 1 cm diameter and about 1.5 mm thickness using a pressure of 5 kN (corresponding to a static pressure of about 100 MPa). The data were recorded as a relative elongation *vs.* temperature.

Kinetic analysis

Kinetic parameters; E, activation energy (kJ mol^{-1}) and A, frequency factor (min^{-1}) were calculated from the non-isothermal TG curves assuming the

Diefallah's composite integral method based on either the modified Coats–Redfern method (composite method I) or Doyle's equation (composite method II) [19–21]. In the Composite method I, the modified Coats–Redfern equation was rewritten in the form:

$$\ln\left[\frac{\beta g(\alpha)}{T^2}\right] = \ln\left(\frac{AR}{E}\right) - \frac{E}{RT} \tag{1}$$

where $g(\alpha)$ is the kinetic model function calculated for the fraction reacted (α) at temperature T and heating rate β. In the Composite method II, Doyle's equation has been rewritten in the form:

$$\log g(\alpha)\beta = \left[\log\frac{AE}{R} - 2315\right] - 0.4567\frac{E}{RT} \tag{2}$$

hence the dependence of $\ln[\beta g(\alpha)/T^2]$ or $\log[\beta g(\alpha)]$ calculated for the different α-values at their respective β-values, on $1/T$ must give rise to a straight master line for the correct form of $g(\alpha)$. A computer program [20] has been devised to perform the data analysis using the different models of heterogeneous solid-state reaction equations [21]. The calculations allow choosing the kinetic mechanism which best fit the data and gives the highest correlation coefficient and the lowest standard deviation. The program also helped calculating the activation energy and the frequency factor from the slope and intercept of the linear fit line. Generally [19], both the Composite methods gave equivalent curves and nearly identical values for the activation parameters.

Two other methods due to Coats–Redfern [22] and Ozawa [23] were also used to calculate the activation parameters assuming the best fit kinetic model obtained from the Composite method. In Coats–Redfern method, the function $g(\alpha)$ is written in the form:

$$-\ln\left[\frac{g(\alpha)}{T^2}\right] = -\ln\frac{AR}{\beta E}\left(1 - \frac{2RT}{E}\right) + \frac{E}{RT} \tag{3}$$

In the Ozawa method the heating rate β was related to the temperature with the equation:

$$-\log\beta = 0.4567\left(\frac{E}{RT}\right) + \text{constant} \tag{4}$$

In the two methods, the activation energy was obtained from the plot of the left hand side term of the equations *vs.* $1/T$. the frequency factor was calculated from the intercept in case of Coats–Redfern method, and using the following equation in case of the Ozawa method:

$$\log A = \log g(\alpha) - \log\left[\frac{E}{\beta R}P\left(\frac{E}{RT}\right)\right] \tag{5}$$

where the function $P(E/RT)$ was approximated by the equation:

$$\log P\left(\frac{E}{RT}\right) = -2.315 - 0.4567\left(\frac{E}{RT}\right) \qquad (6)$$

The obtained activation parameters using the three methods were then compared and discussed.

Results and discussion

Oxidizing atmosphere

Figure 1 shows both the simultaneous TG-EGA curves and DSC curve in presence of air atmosphere at a heating rate of 10°C min^{-1} up to 900°C for the investigated ash. From the figure it is clear that, the ash within this temperature range loses its mass in three well defined steps. The resolution of these steps is not clear enough and can only be realized using IR-EGA and DSC curves.
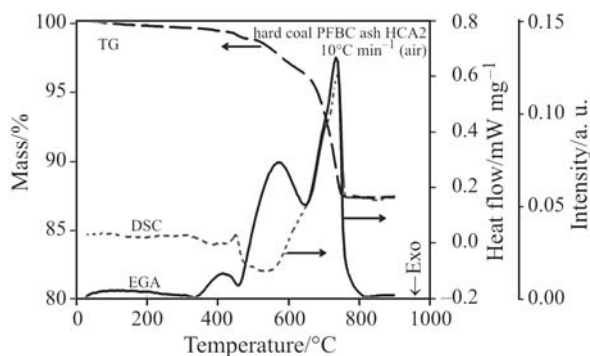

Fig. 1 TG, EGA and DSC curves of HCA2 in air

Paya *et al.* [7] have reported in their study upon different fly ashes obtained from Spanish thermoelectric power plants that the mass loss obtained at 400–450°C was due to water released from the hydrated lime or from the combined water present in the residual clay minerals. They have also pointed out that, the Los Barrios-Cadiz fly ash exhibits a mass loss in the temperature range 430–450°C in spite of the absence of any hydrated lime content. Since the investigated ash contains no hydrated lime (Table 1), thus the first mass loss step at 420–450°C may attributed to the loss of the combined water in the ash.

The anhydrous ash is then thermally stable up to about 510°C. The second decomposition step occurs in the temperature range 510–660°C. It is attributed to the oxidative decomposition of the carbon content of the ash according to the following chemical reaction [7]:

$$2C + xO_2 \rightarrow 2CO_x \ (x=1, 2)$$

The third step starts immediately after the completion of the second one and exhibits the main decomposition percentage of the ash. This step is due to the decomposition of the carbonate content of the ash.

After this decomposition step no excessive mass loss was observed.

Both of the evolution gas and the DSC peaks is closely corresponding to the changes displayed in the TG curve. FTIR analysis of the evolution gas peaks obtained at 430 gives two bands at 3585 and 1510 cm^{-1} characteristic of H$_2$O. The lowering of this bending vibration frequency (1510 cm^{-1}) is attributed to the presence of the water content of the ash in a combined state. The analysis of the other two evolution gas peaks at 575 and 735°C shows two IR bands at 2361 and 685 cm^{-1}. These two bands are assigned to antisymmmetric and bending vibrations of carbon dioxide, respectively. The IR band at 2361 cm^{-1} is considered to be the strongest IR band characteristic of the carbon dioxide [8]. In accordance with the TG results these two peaks are attributed to the evolution of CO$_2$ from the combustion of carbon and decomposition of CaCO$_3$ contents, respectively. The DSC curve shows two endothermic peaks located at 430 and 750°C corresponding to the loss of the combined water and the decomposition of calcium carbonate, respectively. The broad exothermic peak in the temperature range 510–620°C is assigned to the combustion of the carbon content of the ash.

From the TG results it is clear that, the decomposition temperature of the carbonate in the ash is lower than that present in [12, 24]. The reason for this behavior is assigned to the presence of silicon dioxide in the ash components (33%). Dollimore *et al.* [17] have investigated the effect of the addition of silica with different mole ratios on the decomposition temperature of CaCO$_3$ and found that, the decomposition temperature showed a decreasing trend with an increase in the ratio of the silica. They attributed this behavior to the spacing effect of the silica.

Inert atmosphere

Figure 2 shows the TG curve obtained for the decomposition of the ash in flowing N$_2$ atmosphere at a heating rate of 10°C min^{-1} up to 1000°C. From the figure it is obvious that, in an inert environment, carbon oxidation does not take place whereas the mass losses corresponding to the release of the combined water and the carbonate decomposition are still present. Moreover, a steep rising mass loss is observed at >750°C.

It is well known [25] that coal can reduce some minerals (oxides, sulphides…); the most important case is chemical reduction of iron oxide by coke in the blast furnace. Since the investigated ash contains about 9% iron (III) oxide as a mineral phase and at the same time the carbon content of ash has not been oxidized under conditions applied, redox processes may occur between carbon and iron oxide, yielding carbon
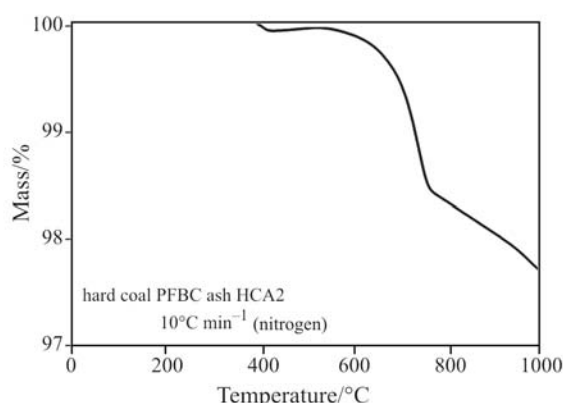
Fig. 2 TG curve of HCA2 in nitrogen

monoxide as carbon oxidation product and resulting in the observed steep mass loss. A similar behavior was reported by Paya *et al.* [7] for fly ashes in the temperature range 700–1100°C. Kanaoka *et al.* [11] have also found a similar behavior for coal fly ash at temperatures higher than 900°C.

Reducing atmosphere

TG, EGA and the DSC curves for the thermal decomposition of the investigated ash in a reducing atmosphere (N_2–H_2 mixture) at a heating rate of 10°C min^{-1} are shown in Fig. 3. The TG curve obtained resembles that obtained on heating under inert atmosphere up to the decomposition step of the carbonate. In contrast to the steep rising mass loss observed under nitrogen atmosphere, a third well defined step is observed under N_2–H_2 condition. This step is also assigned to redox processes involving carbon and iron oxides. This difference in the decomposition behavior in the presence of 2% H_2 may be attributed to that in nitrogen atmosphere the oxidation-reduction reaction is kinetically slow and only go to completion at high temperatures [7], whereas the co-existence of hydrogen seems to enhance the redox process to be completed at a lower temperature.

EGA curve shows a peak in the temperature range 750–960°C in addition to the two peaks, at 425 and 720°C, characteristic for the evolution of com-
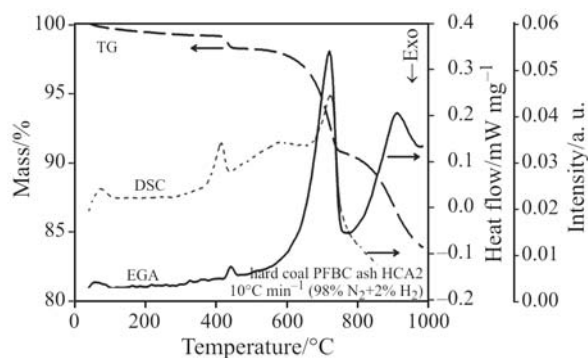

Fig. 3 TG, EGA and DSC curves of HCA2 in N_2–H_2 atmosphere

bined water and carbon dioxide from the decomposition of carbonate, respectively. FTIR analysis of this peak at its maximum temperature (900°C) shows IR band at 2143 cm^{-1}, which can be assigned to stretching vibration of carbon monoxide according to the standard reference data base [18]. This result agrees well with that obtained in the TG results.

DSC curve (Fig. 3) does not show an exothermic peak due to the oxidation of carbon to carbon dioxide and only shows three endothermic peaks. The two peaks at 415 and 725°C assigned as in the case of the air atmosphere to the evolution of the combined water and carbon dioxide (from decomposition of carbonate), respectively. The broad endothermic peak at 573°C can be assigned to the phase transition of the quartz content of the ash according to the following equation [26]:

$$\alpha\text{-quartz} \rightarrow \beta\text{-quartz}$$

The absence of this endothermic peak in the case of decomposition in air is due to the predominance of the strong exothermic oxidation reaction of carbon to carbon dioxide occurring over the same temperature range.
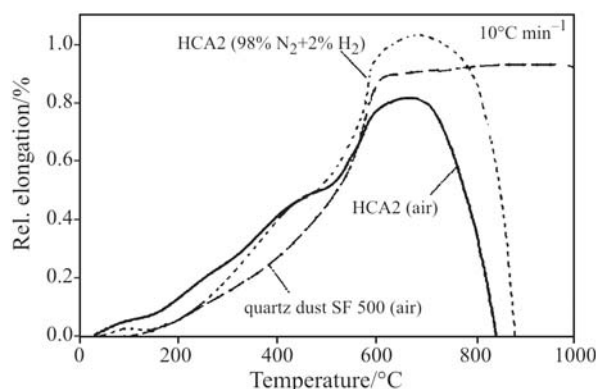

Fig. 4 DIL curves of HCA2 and quartz SF 500

The thermo-mechanical behavior of the ash was studied in air atmosphere and N_2–H_2 mixture. Figure 4 shows the DIL curves obtained for HCA2 in both atmospheres. The DIL curve of quartz SF500 in air atmosphere is also given in Fig. 4 for comparison purposes.

From the figure it is clear that, the behavior of the ash in both atmospheres is the same within the investigated temperature range with the exception that the relative elongation in case of N_2–H_2 mixture larger than that in case of air. The relative elongation was observed to increase slightly with temperature up to about 400°C as a result of the expansion of the sample with temperature increase. Subsequently, the elongation rate was observed to decrease till complete ceasing out near 500°C. At this temperature range the release of the combined water results in a small contraction of the sample which consequently decreases the thermal ex-

pansion rate of the sample. Above this temperature range, the change in the relative elongation of the ash can be assigned to the behavior of the quartz content of the ash (28%) as can be observed from the DIL curve of the pure quartz, in agreement with the DSC results. The change in the slope of the DIL curve at about 573°C is attributed to the volume change resulted from the phase transition of the quartz. This expansion, related to the quartz content of the ash, dominates over the other behaviors occurring, such as the contraction resulting from the oxidative decomposition of the carbon content of the ash at the same temperature range in presence of air atmosphere. The absence of this contraction in the presence of N_2–H_2 mixture results in a pronounced increase in the elongation rate than that observed in air atmosphere. Above 650°C, the ash was observed to undergo a pronounced shrinkage due to the decomposition of calcium carbonate and the sintering of the resulted CaO.

In general, it is obvious that the change of the atmosphere affected the decomposition behavior of the ash. The decomposition temperature of the carbonate content is higher in the presence of air than the other two atmospheres. This behavior will be considered while dealing with the kinetic results of the decomposition reaction. The reason for this difference in the decomposition temperatures may be attributed to the retardation effect of CO_2 gas present in the air atmosphere [27].

Kinetic studies

The effect of changing the surrounded atmosphere on the kinetics of the thermal decomposition reaction of calcium carbonate content of the investigated fly ash was studied under non-isothermal conditions using heating rates of 1, 2, 3, 5 and 10°C min^{-1}, assuming different solid-state reaction equations in view of three integral methods: Composite method [19–21], Coats–Redfern method [22] and Ozawa's method [23].

The thermal decomposition behaviors of the ash under nitrogen and N_2–H_2 atmospheres are nearly the same up to the complete decomposition of the carbonate content and at the same time completely different from that obtained under air atmosphere. The reason for this is attributed to the presence or absence of the carbon in the ash. So, in our kinetic studies we will concentrate on the effect of the carbon content on the kinetics of the carbonate decomposition. We will consider only the kinetic studies in air, in which carbon was oxidized, and in N_2–H_2 mixture, in which carbon is not oxidized.

Typical plots of mass changes (1–α) (at different constant heating rates) *vs.* temperature for the carbonate decomposition step in the investigated ash in air and in N_2–H_2 atmospheres are shown in Fig. 5. Kinetic analysis of the data according to the composite method revealed that the decomposition in air is best described by the Avrami–Erofeev random nucleation growth mechanism (A_2). The phase boundary controlled reaction equations (R_2 and R_3), gave also satisfactory results. In case of N_2–H_2 mixture, the decomposition was found to be best described by the phase boundary controlled reaction equations (R_2 and R_3) and at the same time, the diffusion controlled reaction equations (D_1, D_2, D_3 and D_4) gave satisfactory results. In both atmospheres, the other model equations gave a less satisfactory fit of the data and the exponential law equation (E_1) gave the least fit. Table 2 lists the values of the activation parameters, calculated according to the Composite method based on the Doyle's equation (Composite method II) assuming different heterogeneous solid-state models, for the non-isothermal decomposition of carbonate content of the ash in air and N_2–H_2 mixture. Figure 6 shows the typical results calculated by the composite method

Table 2 Activation parameters of the non-isothermal decomposition of CaCO₃ content of HCA2 in different atmospheres, calculated according to the Composite method II, assuming different kinetic models

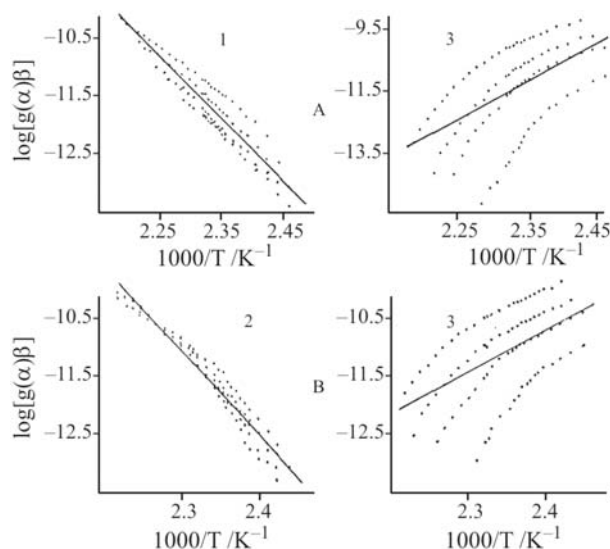| Model	Decomposition of CaCO₃ in air			Decomposition of CaCO₃ in N₂–H₂		
	E/kJ mol^{-1}	log$A$/min^{-1}	r	E/kJ mol^{-1}	log$A$/min^{-1}	r
D$_1$	446±32	22.8±1.9	0.830	283±7	14.4±0.4	0.968
D$_2$	468±33	23.8±1.9	0.829	296±7	15.0±0.5	0.964
D$_3$	495±35	24.9±2.1	0.827	314±9	15.4±0.5	0.958
D$_4$	477±34	23.7±2.0	0.829	302±8	14.7±0.5	0.963
R$_2$	291±12	14.3±0.7	0.932	176±1	8.4±0.1	0.996
R$_3$	297±12	14.6±0.7	0.930	180±2	8.5±0.1	0.996
F$_1$	313±14	16.0±0.8	0.926	189±2	9.5±0.1	0.993
A$_2$	201±3	10.2±0.2	0.990	117±4	5.7±0.2	0.943
A$_3$	171±5	8.3±0.3	0.969	94±5	4.4±0.3	0.869
E$_1$	58±31	4.4±1.8	0.192	16±9	1.3±0.9	0.094
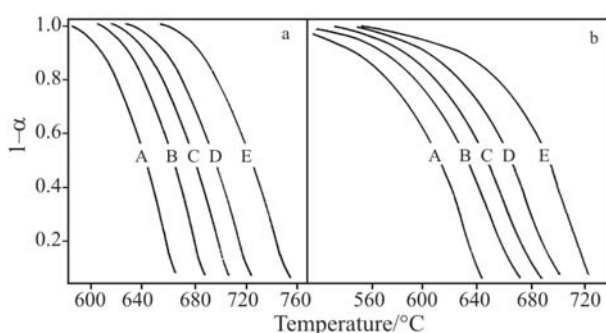
Fig. 5 Dynamic measurements for the non-isothermal decomposition of CaCO$_3$ content of HCA2 in different atmospheres. a – air and b – N$_2$–H$_2$; heating rate: A – 1, B – 2, C – 3, D – 5 and E – 10°C min^{-1}

assuming A$_2$ and E$_1$ models in case of the decomposition in air, and R$_2$ and E$_1$ models in case of the decomposition in N$_2$–H$_2$.

The activation parameters were also calculated on the basis of the Coats–Redfern and Ozawa methods assuming A$_2$ and R$_2$ models for the decomposition in air and N$_2$–H$_2$ mixture, respectively (i.e. the best fit models revealed by the Composite method). The results according to the three computational methods are summarized in Table 3. The reported values of the activation parameters in the case of the Coats–Redfern and the Ozawa methods are the average ones calculated at different heating rates (β) and fractional reaction (α) values, respectively.

The results of the data analysis (Table 3) show a good agreement (within the experimental errors) between the values of the calculated activation parameters. The only exception is the values calculated according to the Coats–Redfern method in the case of the decomposition in air which shows an insignificantly lower value of activation energy than the other two methods. The data also show that, both the integral composite method and the Ozawa method gave the least standard deviation in the calculated experimental parameters.

On comparing the results of the activation parameters obtained at different atmospheres (Table 2), it is clear that, the values of the calculated activation parameters assuming the different models in case of N$_2$–H$_2$ atmosphere are nearly half that obtained in the

Fig. 6 Composite analysis of TG data for the non-isothermal decomposition of CaCO$_3$ content of HCA2 in different atmospheres based on Doyle's equation assuming: 1 – A$_2$ model, 2 – R$_2$ model and 3 – E$_1$ model. A – air atmosphere, B – N$_2$–H$_2$ atmosphere

air atmosphere. This can be attributed to the presence of the unburned carbon during the thermal decomposition of carbonate in N$_2$–H$_2$ atmosphere. The unburned carbon acts as a spacer causing a fewer points of contact between particles of calcium carbonate and increases the interfaces which facilitate the decomposition and decrease the activation energy.

The changing of the reaction mechanism for the decomposition of carbonate with the atmosphere is also related to the presence or absence (due to the oxidation) of the carbon. The absence of carbon in case of the decomposition in air causes more points of contact between the carbonate particles which allows more chances of formation of nucleation. This agrees well with the obtained (A$_2$) model in which the reaction is controlled by initial random nucleation followed by overlapping growth in two dimensions. The increase in the interface between the carbonate particles in the case of the presence of carbon (in N$_2$–H$_2$ mixture) enhance the application of the (R$_2$) model in which an interface moves at constant velocity and nucleation occurs virtually instantaneously.

Table 3 Activation parameters of the non-isothermal decomposition of CaCO$_3$ content of HCA2 in different atmospheres, calculated according to the different computational methods indicated

Method	Decomposition of CaCO$_3$ in air (A$_2$ model)		Decomposition of CaCO$_3$ in N$_2$–H$_2$ (R$_2$ model)	
	E/kJ mol^{-1}	log$A$/min^{-1}	E/kJ mol^{-1}	log$A$/min^{-1}
Composite II	201±3	9.8±0.4	176±1	8.4±0.1
Coats–Redfern	182±15	9.7±0.5	167±10	7.9±0.6
Ozawa	208±2	9.8±0.4	183±1	8.0±0.1

Conclusions

TG, IR-EGA, DSC and DIL studies of the thermal decomposition of hard coal ash (HCA2) show that changing of the surrounding atmosphere has pronounced effects on the thermal behavior. In air, the carbon content of the ash was oxidized to carbon dioxide before the decomposition of carbonate content. In N_2 or in N_2–H_2, an oxidation-reduction reaction occurs between the carbon content and the iron oxide following the carbonate decomposition. This reaction is kinetically slow and only goes to completion at high temperatures in nitrogen atmosphere, while in N_2–H_2, the reducing effect of H_2 enhances the reaction. The non-isothermal kinetics of the carbonate decomposition in air or N_2–H_2, according to the Composite method, show that the change of the atmosphere, in other words the presence or absence of the carbon, alters the reaction mechanism for the decomposition and, consequently, the values of the activation parameters.

References

1 K. S. Grochawiak, J. Golas, H. Jankowski and S. Kozinski, Fuel, 83 (2004) 1847.
2 O. E. Manz, Fuel, 78 (1999) 133.
3 U. M. Graham, Fuel, 76 (1997) 689.
4 M. J. McCarthy and R. K. Dhir, Fuel, 80 (2001) 1659.
5 W. Roszczynialski and W. N. Wczelik, J. Therm. Anal. Cal., 77 (2004) 151.
6 V. Rahhal and R. Talero, J. Therm. Anal. Cal., 87 (2004) 191.
7 J. Paya, J. Monzo, M. V. Borrachero, E. Perris and F. Amahjour, Cem. Concr. Res., 28 (1998) 675.
8 P. Fermo, F. Cariati, S. Satacesaria, S. Bruni, M. Lasagni, M. Tettamanti, E. Collina and D. Pitea, Environ. Sci. Technol., 34 (2000) 4370.
9 M. Fan and R.C. Brown, Energy Fuels, 15 (2001) 15.
10 G. H. Hemmer, D. Hoff and G. Kasper, Adv. Powder Technol., 14 (2003) 631.
11 C. Kanaoka, M. Hata and H. Makino, Powder Technol., 118 (2001) 107.
12 M. Maciejewski, Thermochim. Acta, 355 (2000) 145.
13 J. H. Khinast, G. F. Krammer, Ch. Brunner and G. Staudinger, Chem. Eng. Sci., 51 (1996) 623.
14 J. M. Criado, M. Gonzalez, J. Malek and A. Ortega, Thermochim. Acta, 254 (1995) 121.
15 Y. Wang and W. J. Thomson, Chem. Eng. Sci., 50 (1995) 1373.
16 J. P. Sanders and P. K. Gallagher, Thermochim. Acta, 388 (2002) 115.
17 D. Dollimore, P. Tong and K. S. Alexander, Thermochim. Acta, 282/283 (1996) 13.
18 NIST Chemistry Web Book, Standard reference data base No. 69–March 2003.
19 El-H. M. Diefallah, Thermochim. Acta, 202 (1992) 1.
20 El-H. M. Diefallah, A. Y. Obaid, A. H. Qusti, A. A. El-Bellihi and A. M. Abdel Wahab, Thermochim. Acta, 274 (1996) 172.
21 M. A. Gabal, Thermochim. Acta, 412 (2004) 55.
22 E. Urbanovici, C. Popescu and E. Segal, J. Therm. Anal. Cal., 58 (1999) 683.
23 J. H. Flynn, Thermochim. Acta, 282/283 (1996) 35.
24 C. K. Hsu, Thermochim. Acta, 392–393 (2002) 157.
25 R. A. Higgins, Engineering Metallurgy, 2nd Ed. Vol. 1, ELBS, London 1974.
26 T. Hatakeyama and Z. Liu, Handbook of Thermal Analysis, Wiley, Weinheim 1998.
27 B. V. L'Vov, L. K. Polzik and V. L. Ugolkov, Thermochim. Acta, 390 (2002) 5.